ir reflectance spectra of Ti_2O_3: Infrared-active phonons and Ti 3d electronic effects

G. Lucovsky, R. J. Sladek,*† and J. W. Allen
Xerox Palo Research Center, Palo Alto, California 94304
(Received 9 August 1977)

The room-temperature reflectance of Ti_2O_3 has been measured between 50 and 4000 cm^{-1} for the two principal polarizations, E perpendicular and E parallel to the c axis. An analysis of the data provides (i) the properties of the ir-active long-wavelength phonons—TO- and LO-phonon frequencies, oscillator strengths, and the damping; (ii) the values for the optical frequency ϵ_∞ and quasistatic ϵ_0 dielectric constants, and (iii) information about electronic effects associated with the partially occupied Ti 3d states. The latter include the anisotropy in the free-carrier electronic conductivity $\sigma_\perp/\sigma_\parallel$ and the energy separation between the lowest-lying d levels. Comparisons are made with the phonon properties of other α-corundum structured sesquioxides α-Al_2O_3 and Cr_2O_3.

I. INTRODUCTION

Many of the studies of Ti_2O_3 have emphasized the semiconductor-semimetal transition that occurs between 400 and 550 °K.[1] It has been shown that the "approach," with increasing temperature, and subsequent energy overlap of the lowest-lying Ti 3d levels, can account for: (i) changes in the electronic conductivity, (ii) a maximum in the heat capacity, and (iii) an anomalous temperature dependence in certain elastic constants. Large and temperature-dependent phonon anharmonicity is inferred from ultrasonic[2] and piezoresistance[3] measurements. The Raman-active phonons of Ti_2O_3 have been shown to display shifts in frequency in the temperature regime of the conductivity transition.[4,5] This paper reports the first studies of the room-temperature ir reflectance of Ti_2O_3 for the two principal polarizations. A subsequent paper will address the temperature dependence. We deduce the frequency dependence of the dielectric functions, identifying contributions from: (i) the ir-active phonons, (ii) the low-mobility charge carriers in the energy levels derived from the Ti 3d atomic states, and (iii) an interband electronic transition involving the same Ti 3d states.

Ti_2O_3 has the α-corundum (α-Al_2O_3) crystal structure with symmetry D_{3d}^6 ($R\bar{3}c$).[6] A group-theoretical analysis predicts six ir-active long-wavelength modes in addition to the seven Raman-active modes, $2A_{1g}+5E_g$: two A_{2u} modes with polarization parallel to the crystalline c axis ($\vec{E}\|\vec{c}$) and four E_u modes with polarization perpendicular to the c axis ($\vec{E}\perp\vec{c}$). The properties of these ir modes have been identified in α-Al_2O_3,[6] and purportedly for Cr_2O_3.[7] We have found some serious errors in the frequency assignments for Cr_2O_3,[8] and we include in this paper new results obtained by us for Cr_2O_3 which help provide for an informative comparison with the corresponding phonon properties of Ti_2O_3 and α-Al_2O_3. Studies of the reflectance of V_2O_3 (α-corundum phase) have not yielded the properties of the ir phonons due to the high metallic conductance[9-11]; however, the frequencies of two of the ir phonons for $\vec{E}\perp\vec{c}$ in $(V_{0.988}Cr_{0.012})_2O_3$ have been identified.[9]

At temperatures near 300 °K, Ti_2O_3 is believed to be an intrinsic p-type semiconductor with an energy gap of approximately 0.1 eV separating the valence band from a narrower conduction band. The valence and conduction bands are derived principally from the Ti 3d atomic states.[12] The lowest-lying atomic d states are split into a_{1g} orbitals directed between the pairs of Ti atoms lying along the c axis, and e_g^π orbitals directed toward Ti atoms lying in the puckered basal plane perpen-

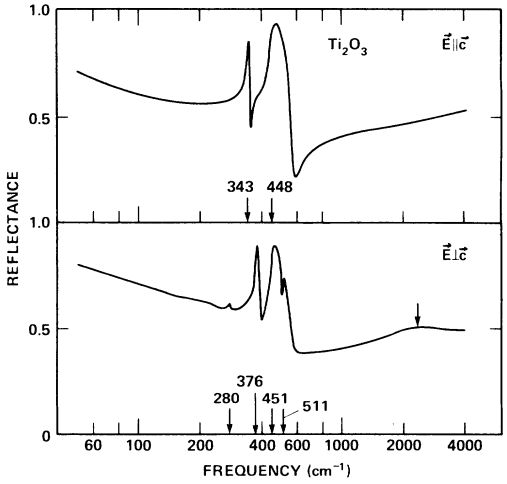

FIG. 1. Room-temperature ir-reflectance spectra for Ti_2O_3 for $\vec{E}\|\vec{c}$ and $\vec{E}\perp\vec{c}$. The arrow in the figure for $\vec{E}\perp\vec{c}$ indicates a feature we assign to an electronic transition. The sharper features in both polarizations at lower wave numbers are due to phonons. The markers give the TO-phonon frequencies derived from the oscillator analysis.

dicular to the c axis. The relative energies, and hance occupation of these states in Ti_2O_3 and V_2O_3,[12,13] in $(Ti_{1-x}V_x)_2O_3$ and $(V_{1-x}Cr_x)_2O_3$,[1] and in Cr_2O_3,[12] have been used to account for the observed differences in the conductivity type and in the c/a lattice-parameter ratio. For example, in Ti_2O_3 the empty e_g^π levels lie above the occupied a_{1g} levels yielding a narrow-band-gap semiconductor with a small c/a ratio, 2.65; in contrast, the level ordering is reversed with considerable overlap of the a_{1g} and e_g^π bands in V_2O_3 which exhibits a metallic conducitivity with a larger c/a ratio, 2.83. In Cr_2O_3, the electrons occupy localized a_{1g} and e_g^π levels, and the crystal is insulating. Interband electronic transitions at photon energies in excess of about 0.7 eV have been studied in Ti_2O_3 by means of optical reflectance[14,15] and also through resonance Raman scattering.[14,16] Our measurements extend to much lower photon energies, from ~0.5 eV (or 4000 cm^{-1}) to ~0.0062 eV (or 50 cm^{-1}) and identify an additional electronic d-level transition giving further support to the one-electron energy-level model discussed above.[12,13]

II. EXPERIMENTAL RESULTS AND DATA ANALYSIS

The reflectance measurements were made on a single crystal sample of Ti_2O_3 obtained from a boule grown at the Central Crystal Growth Facility at Purdue University. The spectra for the two polarizations were obtained using a Perkin Elmer Model 180 double-beam Spectrophotometer equipped with wire-grid ir polarizers. Measurements were made on a polished and oriented face containing the crystalline c axis with the polarization perpendicular to the plane of incidence. This reflection geometry minimizes any mixing of the ir response functions.[6,17] The crystal temperature, established within the N_2-purged instrument sampling chamber by the incident radiation, was approximately 35 °C.

Figure 1 gives the wave-number dependence of the reflectance for the two polarizations. The relatively sharp features below about 600 cm^{-1} are due to the ir-active phonons. As anticipated from the group theory analysis,[6] there are two features for $\vec{E} \| \vec{c}$ and four for $\vec{E} \perp \vec{c}$. The markers on the wave-number axis indicate the frequencies of the TO phonons as deduced from the oscillator analysis. Other features are also evident in the reflectance spectra. The broad maximum between 1500 and 3000 cm^{-1} in the $\vec{E} \perp \vec{c}$ spectrum is assigned to an electronic interband transition between a_{1g} and e_g^π Ti $3d$ states. The rising reflectance at very low wave numbers and the relatively high reflectance at the high wave-number side of the dominant restrahlen bands (at ~ 600 cm^{-1} in both polarizations) are due to mobile charge carriers in the Ti $3d$ bands. In contrast, for the insulating crystals α-Al_2O_3,[6] and Cr_2O_3,[7,8] the reflectance is essentially constant for low wave numbers below the lattice bands and very nearly zero at the high-frequency edge of the strongest reststrahlen bands.

Two techniques were used to analyze the reflectance data: a preliminary Kramers-Kronig (KK) analysis and then an oscillator fit. The KK analysis is used to estimate the starting values for an iterative search for the oscillator parameters. The dielectric function $\epsilon(\nu)$ is constructed as the sum of the two frequency-dependent terms: a lattice contribution $\epsilon^{\rm lat}(\nu)$ (which is a summation over phonon modes), and a free carrier or Drude contribution, $\epsilon^{\rm fc}(\nu)$. The contribution from electronic interband transitions between 1500 and 3000 cm^{-1} in the $\vec{E} \perp \vec{c}$ spectrum is identified in the KK analysis, but cannot be treated in any convenient way in the oscillator analysis. The dielectric function is then given by

$$\epsilon(\nu) = \epsilon_\infty + \epsilon^{\rm lat}(\nu) + \epsilon^{\rm fc}(\nu), \tag{1}$$

where ϵ_∞ is an optical frequency dielectric constant which reflects the contributions from the higher photon-energy electronic interband transitions. We neglect a small frequency-dependent component in ϵ_∞. The lattice contribution is given by

$$\epsilon^{\rm lat}(\nu) = \sum \frac{S_i \nu_i^2}{\nu_i^2 - \nu^2 - i\gamma_i \nu}, \tag{2}$$

where S_i is the oscillator strength and contribution of the lattice mode to a quasistatic dielectric constant, ν_i is the TO phonon frequency (in cm^{-1}) and γ_i an empirical damping constant (also given in cm^{-1}). The sum is over four modes for $\vec{E} \perp \vec{c}$, and two for $\vec{E} \| \vec{c}$. It is often more convenient to consider the damping relative to ν_i, so that γ_i/ν_i is then a dimensionless damping parameter. The free-carrier term is given by

$$\epsilon^{\rm fc}(\nu) = -\nu_p^2/\nu(\nu + iG_p), \tag{3}$$

where ν_p^2 is a term proportional to the free-carrier density (in effect an unscreened plasma frequency, the plasma frequency in the absence of phonons is $\nu_p/\epsilon_\infty^{1/2}$), and G_p is the damping (both ν_p and G_p are in cm^{-1}). ν_p^2 is related to the free-carrier density N_0 by

$$(2\pi c)^2 \nu_p^2 = 4\pi N_0 e^2/m^*, \tag{4}$$

where m^* is the free-carrier effective mass. G_p is related to a scattering time τ by

$$(2\pi c) G_p = 1/\tau. \tag{5}$$

The free-carrier mobility is then given by $\mu = e\tau/m^*$.

Table I summarizes the results of the analysis.

TABLE I. Oscillator fit and derived parameters for phonons and plasmons in Ti_2O_3. Included from the oscillator fit for the phonons are ν_{TO}, the TO-phonon frequency; S, the oscillator strength; γ/ν_{TO}, the relative damping; and ϵ_∞, the optical-frequency dielectric constant. The derived parameters include e_T^*/e, a macroscopic infrared effective charge; ν_{LO}, the "bare" LO-phonon frequency; and ϵ_0, a quasistate dielectric constant defined in the absence of free carriers. For the plasmons the fit parameters are ν_p, an unscreened plasma frequency [see Eqs. (1), (3), and (4)] and G_p, a damping frequency. The derived parameters are $\sigma^{opt}(\nu \to 0)$, an optical conductivity extrapolated to zero frequency, $N_0/(m^*/m_0)$, a ratio of the free-carrier density to an effective electronic mass, and $\mu(m^*/m_0)$, a product of a mobility and carrier mass.

		Phonons						
Symmetry		Oscillator fit				Derived		
		ν_{TO} (cm^{-1})	S	γ/ν_{TO}		ν_{LO} (cm^{-1})	e_T^*/e	
$\vec{E}\perp\vec{c}$	1	280	0.15	0.012	$\epsilon_\infty=31.2$	281	0.23	$\epsilon_\infty=45.8$
	2	376	5.15	0.012		391	1.84	
	3	451	8.88	0.025		502	2.90	
	4	511	0.43	0.025		537	0.72	
$\vec{E}\parallel\vec{c}$	1	343	3.0	0.010	$\epsilon_\infty=27.7$	351	1.28	$\epsilon_0=44.1$
	2	448	13.4	0.032		552	3.52	

	Plasmons				
	ν_p (cm^{-1})	G_p (cm^{-1})	$\sigma^{opt}_{\nu\to0}$ (Ω^{-1} cm^{-1})	$N_0/(m^*/m_0)$ (cm^{-3})	$\mu(m^*/m_0)$ (cm^2/v sec)
$\vec{E}\perp\vec{c}$	2.81×10^3	766	172.0	8.81×10^{19}	12.2
$\vec{E}\parallel\vec{c}$	1.52×10^3	507	75.5	2.57×10^{19}	18.4

We include in the table the values of ϵ_∞, $\nu_i(=\nu_{TO})$, S_i, γ_i/ν_i, ν_p, and G_p as obtained from the oscillator analysis, as well as other parameters that are derived from those given above. The first of these is an infrared effective charge $(e_T^*/e)_i$ that is calculated from the relation

$$(e_T^*/e)_i = 1.43\times10^8[(\bar{m}S_i)^{1/2}\nu_i]/N^{1/2}, \qquad (6)$$

where $\bar{m}$ is a mode mass, taken to be $\bar{m}^{-1}=2m_{Ti}^{-1}+3m_O^{-1}$, and N is an oscillator density, the number of Ti_2O_3 units/cm^3.

We next consider the longitudinal excitations. In a system without free carriers, these are the longitudinal optic phonons and their frequencies are identified by the positions of the peaks in the energy-loss function $-\mathrm{Im}[1/\epsilon(\nu)]$. However, in a system with free carriers, the peaks in $-\mathrm{Im}[1/\epsilon(\nu)]$ define the frequencies of coupled plasmon–LO-phonon modes. To illustrate the effects of free carrier or plasma modes on the dielectric functions, consider first the imaginary part of $\epsilon(\nu)=\epsilon_1+i\epsilon_2$. Figure 2 includes $\epsilon_2(\nu)$ for the two polarizations, $\vec{E}\perp\vec{c}$ in Fig. 2(a) and $\vec{E}\parallel\vec{c}$ in Fig. 2(b). The dashed portion of each of the curves includes the contribution from both types of excitations, whereas the solid portion is due solely to the free carriers. The contributions to ϵ_2 are additive so that the peaks in $\epsilon_2(\nu)$ have the same positions they would have in the absence of the free carriers. This is the case since the phonon features are very sharp, whereas the free-carrier contribution displays a power law response over a broad range of frequency. The changes in the energy loss function are on the other hand more striking.

Figures 3(a) and 3(b) give the energy-loss func-

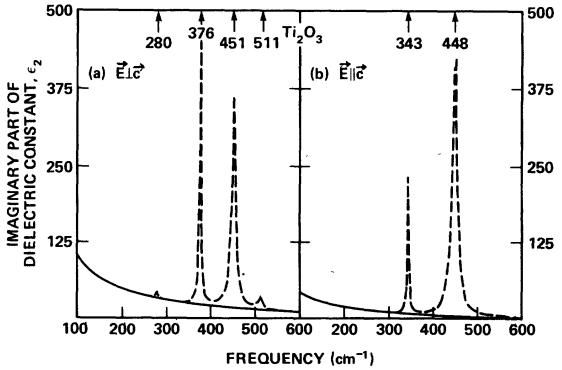

FIG. 2. ϵ_2 spectra for Ti_2O_3: (a) $\vec{E}\perp\vec{c}$; (b) $\vec{E}\parallel\vec{c}$. The dashed curve is the total ϵ_2 function as synthesized from the oscillator parameters given in Table I. The solid curve is the contribution from the free carriers. The markers identify the frequencies of the TO phonons.

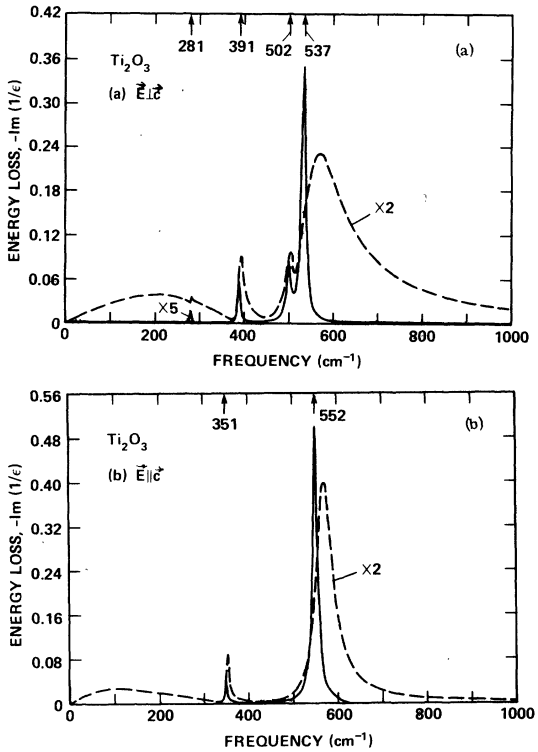

FIG. 3. Energy-loss spectra $[-\mathrm{Im}(1/\epsilon)]$ for Ti_2O_3: (a) $\vec{E}\perp\vec{c}$ and (b) $\vec{E}\parallel\vec{c}$. The dashed curve is the total energy-loss function; the maxima in these functions give the frequencies of the coupled LO-phonon–plasmon modes. The solid curves are the contributions from the phonons alone. The markers indicate frequencies for these "bare" LO phonons.

tions for the respective polarizations, $\vec{E}\perp\vec{c}$, and $\vec{E}\parallel\vec{c}$. The dashed curve is the contribution from both excitations and the solid curve is the contribution from the phonons alone. The phonon contribution is obtained by setting $\nu_p = 0$ in Eq. (3) so that the positions of the peaks in the solid curves are then the frequencies of "bare" LO phonons. These are listed in Table I. Note further that there are five maxima in the *total* energy loss function for $\vec{E}\perp\vec{c}$, one more than the number of phonon modes, and in a corresponding way there are three peaks in the *total* energy-loss function for $\vec{E}\parallel\vec{c}$. For $\vec{E}\perp\vec{c}$, three of these peaks are sharp and very close to the "bare" LO-phonon peaks, whereas the other two peaks are considerably broader and at different frequencies. The broad highest frequency peak is at a frequency in excess of the highest frequency "bare" LO phonon, and the very broad low-frequency peak lies well below the lattice modes. A similar situation prevails for the other polarization. These two broad features contain the strongest plasmon contributions; this is reflected in their linewidth.

The next derived entry in the table is a value for a *quasistatic* dielectric constant ϵ_0, which is defined by the relation

$$\epsilon_0 = \epsilon_\infty + \sum S_i \tag{7}$$

and is the static dielectric constant in the absence of free carriers. The "bare" LO-phonon frequencies and the ϵ_0 are useful for making comparisons with other α-corundum structured crystals. In addition they satisfy the Lydanne-Sach-Teller (LST) relation as it applies to crystals with more than one ir-active mode. In a crystal with only one ir-active mode, the ratio of the LO- and TO-phonon frequencies can be related to the ratio of dielectric constants, $\epsilon_0/\epsilon_\infty$, by

$$(\nu_{LO}/\nu_{TO})^2 = \epsilon_0/\epsilon_\infty . \tag{8}$$

This is derived by noting that in the absence of damping [$\gamma_i = 0$ in Eq. (2)], the LO-phonon frequency satisfies the relation

$$\epsilon_\infty + S\nu_T^2/(\nu_T^2 - \nu_L^2) = 0. \tag{9}$$

Combining this expression with the definition of ϵ_0 ($\equiv\epsilon_\infty + S$), one obtains Eq. (8). The extension to a multiphonon system is straighforward; in the limit of small damping, $\gamma_i/\nu_i \ll 1$, the LO-phonon frequencies are solutions of

$$\epsilon_\infty + \sum S_i \nu_T^2(i)/[\nu_T^2(i) - \nu_L^2(i)] = 0 , \tag{10}$$

and the extended LST relation[18] is then given by

$$\epsilon_0/\epsilon_\infty = \prod_i [\nu_L(i)/\nu_T(i)]^2 . \tag{11}$$

This relation [Eq. (11)] is satisfied for both polarizations in Ti_2O_3; for $\vec{E}\perp\vec{c}$, $\epsilon_0/\epsilon_\infty = 1.47$ and $\prod_i[\nu_L(i)/\nu_T(i)]^2 = 1.48$, whereas for $\vec{E}\parallel\vec{c}$ both quantities are equal to 1.59. The fact that the values we have obtained for ϵ_0 and the $\nu_L(i)$ satisfy Eq. (11) supports the validity of our approach of defining these parameters in the absence of free carriers.

The final entries in the table give the properties of the plasmons. In addition to ν_p and G_p, we include values for the optical conductivity as $\nu \to 0$. Chen and Sladek[3] have obtained the dc conductivity for the two polarizations, $\sigma_\perp^{dc} = 143\ \Omega^{-1}\,\mathrm{cm}^{-1}$ and $\sigma_\parallel^{dc} = 55\Omega^{-1}\,\mathrm{cm}^{-1}$. The conductivities obtained from the oscillator analysis are in good agreement with the dc measurements. We cannot, however, obtain separate values for N_0, the mobile carrier concentration, or μ, the mobility. We therefore give $N_0/(m^*/m_0)$ and $\mu(m^*/m_0)$ which can then be compared with dc measurements once a value for m^* is obtained; m_0 is the free-electron mass. The dc conductivity measurements of Chen and Sladek[3] in-

dicate a significant anisotropy in the conductivity $\sigma_{\perp}^{dc}/\sigma_{\parallel}^{dc} = 2.6$. A similar anisotropy is deduced from our optical studies, $\sigma_{\perp}^{opt}/\sigma_{\parallel}^{opt} = 2.3$. We have also studied alloys in the system Ti_2O_3-V_2O_3 for concentrations up to 10% V_2O_3,[19] and find similar values for the anisotropy of the optical conductivity near room temperature.

III. DISCUSSION

There are two aspects of the ir-reflectance results that we consider: (i) a comparison of the properties of the ir-active phonons in Ti_2O_3 with those of α-Al_2O_3 and Cr_2O_3 and (ii) the assignment of the broad maximum in the $E \perp c$ spectrum of Ti_2O_3 between 1500 and 3000 cm^{-1}.

Table II compares the phonon properties of Ti_2O_3, α-Al_2O_3,[6] and Cr_2O_3.[8] We include in the comparison the TO- and LO-phonon frequencies, the phonon contributions to the dielectric constant, and values for the static- and optical-frequency dielectric constants. These comparisons indicate systematic trends with the values for Cr_2O_3 generally being in between those for α-Al_2O_3 and Ti_2O_3. For example, for the phonon frequencies, the trend is

$$[\nu_{TO}(i)]_{\alpha\text{-}Al_2O_3} > [\nu_{TO}(i)]_{Cr_2O_3} > [\nu_{TO}(i)]_{Ti_2O_3}, \quad (12)$$

whereas the trend in ϵ_∞ (and also ϵ_0) is in the opposite sense, i.e.,

$$[\epsilon_\infty^{\perp,\parallel}]_{Ti_2O_3} > [\epsilon_\infty^{\perp,\parallel}]_{Cr_2O_3} > [\epsilon_\infty^{\perp,\parallel}]_{\alpha\text{-}Al_2O_3}. \quad (13)$$

It is tempting to try to make more quantitative comparisons among these materials; however, this can be done only with considerable uncertainty. Consider first the phonon frequencies. They can always be expressed in the form

$$\nu^2 = k/\bar{m}, \quad (14)$$

where k is an effective force constant and $\bar{m}$ is a mode or oscillator mass. We would like to associate the highest-frequency phonon for each polarization with a rigid-lattice mode in which the metal and oxygen ions move in opposite directions, along the c axis for the A_{2u} modes and in the basal plane for the E_u modes. For these modes, in a crystal of M_2O_3, $\bar{m}^{-1} = 2m_M^{-1} + 3m_O^{-1}$. Therefore a comparison of $\bar{m}\nu^2$ yields the relative values of k. Consider first the A_{2u} modes: if we assume a rigid sublattice mode character for the higher frequency A_{2u} mode, then we find

$$k_{\alpha\text{-}Al_2O_3} \sim k_{Cr_2O_3} > k_{Ti_2O_3}. \quad (15)$$

It is difficult, however, to relate the relative values of k to any microscopic parameters because they contain contributions from both short-range bonding forces and longer-range Coulomb and dipole-dipole interactions.[20] A further complication in these comparisons is revealed in the relative oscillator strengths of the two A_{2u} modes. For Ti_2O_3 and Cr_2O_3, the higher-frequency mode is stronger, whereas in α-Al_2O_3, the reverse is true. Similar problems arise in comparison of E_u modes. These effects can be understood on the basis of the different electronic structures of the materials as will be seen below.

Consider first the application of an ionic model to α-Al_2O_3. The band gap approximately 7 eV, is then between occupied p states associated with the O^{2-} ions and empty s states associated with the Al^{3+} ions. The properties of α-Al_2O_3 suggest additional covalent contributions to the bondings so that it is more appropriate to label the states as bonding (σ) and anti-bonding (σ^*). In the transition-metal sesquioxides, the d states of the metal atoms yield additional states in the gap between the σ and σ^*

TABLE II. Comparison of phonon frequencies, oscillator strengths, and optical-frequency and static dielectric constants for Ti_2O_3, Cr_2O_3 and α-Al_2O_3.

Symmetry		Ti_2O_3			Cr_2O_3			α-Al_2O_3		
$\vec{E} \perp \vec{c}$		$\epsilon_\infty = 31.2$		$\epsilon_0 = 45.8$	$\epsilon_\infty = 5.73$		$\epsilon_0 = 10.33$	$\epsilon_\infty = 3.2$		$\epsilon_0 = 9.5$
E_u		ν_{TO} (cm^{-1})	ν_{LO} (cm^{-1})	S	ν_{TO} (cm^{-1})	ν_{LO} (cm^{-1})	S	ν_{TO} (cm^{-1})	ν_{LO} (cm^{-1})	S
	1	280	281	0.15	305	306	0.12	385	388	0.30
	2	376	391	5.15	440	442	0.18	442	480	2.7
	3	451	502	8.88	538	593	3.75	569	625	3.0
	4	511	537	0.43	609	734	0.55	635	900	0.30
$\vec{E} \parallel \vec{c}$		$\epsilon_\infty = 27.7$		$\epsilon_0 = 44.1$	$\epsilon_\infty = 5.97$		$\epsilon_0 = 11.93$	$\epsilon_\infty = 3.1$		$\epsilon_0 = 11.64$
A_{2u}		ν_{TO} (cm^{-1})	ν_{LO} (cm^{-1})	S	ν_{TO} (cm^{-1})	ν_{LO} (cm^{-1})	S	ν_{TO} (cm^{-1})	ν_{LO} (cm^{-1})	S
	1	343	351	3.0	402	417	1.36	400	512	6.8
	2	448	552	13.4	533	726	4.60	583	871	1.7

states. A one-electron energy level model for these d states has been proposed by Goodenough and applied to Ti_2O_3 and Cr_2O_3.[12,13] The details of the model are discussed in the references; here we include a schematic representation of the energy levels of the d electrons in Fig. 4. The lowest $3d$ energy gap in Ti_2O_3 is between a_{1g} and e_g^π states and at room temperature is believed to be ~0.1 eV.[1,12,13] We identify the broad maximum between 1500 and 3000 cm^{-1} in the $\vec{E}\perp\vec{c}$ spectrum with $a_{1g}\rightarrow e_g^\pi$ transitions. The low-energy side of this absorption band might extend down to 1200 cm^{-1} or 0.1 eV, as required by the conductivity activation energy. Across the gap, $a_{1g}\rightarrow e_g^\pi$ transitions are allowed for $\vec{E}\perp\vec{c}$, but forbidden for $\vec{E}\parallel\vec{c}$, consistent with our observations. Recently there have been several band-structure calculations for Ti_2O_3 and V_2O_3, a simplified model calculation by Nebenzahl and Weger[21] and a more elaborate calculation by Ashkenazi and Chuchem.[22] The calculations indicate mixing of the $3d$ states, in this respect the one-electron model of Goodenough may be an approximation to the real electronic structure. Nonetheless, comparisons of the calculated densities of states for Ti_2O_3 and V_2O_3 (see Figs. 7, 8, and 11 of Ref. 22) with the one-electron model indicate considerable qualitative agreement between these two approaches. Further, Ashkenazi and Chuchem obtain a gap in Ti_2O_3 only by introducing Coulomb interactions in an approximate way which leads to the number of occupied e_g^π states being 0 at zero temperature. We therefore use the Goodenough one-electron model, which

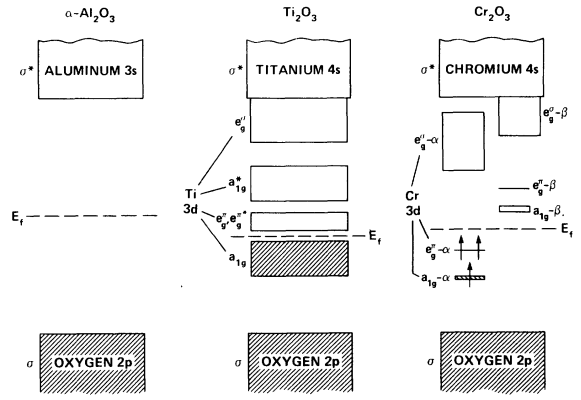

FIG. 4. Schematic representation of the electronic energy states near the optical band gap in α-Al_2O_3, Ti_2O_3 and Cr_2O_3. The d states of Ti_2O_3 and Cr_2O_3 are labeled to reflect their atomic orbital parentages and crystalline field splittings according to the one electron model of Goodenough (Refs. 12, 13.) Bands of nonlocalized d states occur in Ti_2O_3, while in Cr_2O_3 the d states are localized and subdivided into α and β states of opposite spin polarizations. E_f is the Fermi energy.

preserves the a-like and e-like character of the $3d$ states, as a basis for the comparison of the phonon properties of α-Al_2O_3, Ti_2O_3, and Cr_2O_3.

The Cr^{3+} ion contains three d electrons, which occupy the lowest-lying a_{1g} and e_g^π states. The minimum optical band gap is associated with a spin-flip transition. The d electrons in Cr_2O_3 are considerably more localized than in Ti_2O_3, and the lowest-energy optical excitations have a Frenkel excitaton character. These excitons greatly resemble $d\rightarrow d$ transitions of the Cr^{3+} ion and begin at about 1.7 eV.[23]

The properties of the optic phonons and dielectric constants can then be related to this simplified one-electron energy-level scheme. Consider first the relative values of the optical-frequency dielectric constants ϵ_∞. The systematic increases from an average value of ~3 in Al_2O_3, to ~6 in Cr_2O_3 and finally to ~30 in Ti_2O_3, reflect the corresponding decreases in the minimum band gap. The very large increase between Cr_2O_3 and Ti_2O_3 also reflects the very different nature of the excited hole-electron states, highly localized in Cr_2O_3 as compared to very nearly itinerant in Ti_2O_3. The relative values of the total lattice polarizabilities $\sum S_i$, also have their origin in the nature of the lowest-lying electronic excitations. For example, dynamic contributions to e_T^*/e and hence S_i also scale as the reciprocal of the average band gap, and hence as ϵ_∞.[24] This property of the phonons is similar in Cr_2O_3 and α-Al_2O_3, but markedly different in Ti_2O_3. Finally, the softening of effective force constants for the rigid sub-lattice modes in Ti_2O_3 relative to Cr_2O_3 and α-Al_2O_3 [see Eq. 15] is also related to electronic contributions from the highly polarizable Ti $3d$ states.

The one-electron energy-level model for the d states can also be used to explain the differences in the oscillator strengths of the individual phonon modes. Consider first the E_u modes for $\vec{E}\perp\vec{c}$. We have labeled the modes in the Table II as 1, 2, 3, and 4, in order of increasing frequency. Consider first Ti_2O_3 and α-Al_2O_3. Note that the relative strengths of the modes follow essentially the same pattern. The strongest mode is number 3, with 2 being next in strength. In contrast, modes 1 and 4 are considerably weaker, by about an order of magnitude. The situation in Cr_2O_3 is markedly different. Mode 3 is dominant as in α-Al_2O_3 and Ti_2O_3; however, all of the three other modes are considerably weaker. One possible explanation for these differences may lie in the occupancy of the transition metal d states. In Ti_2O_3 (and of course in α-Al_2O_3, as well) the e_g^π levels are not occupied (at least at 0 °K). In contrast, in Cr_2O_3 these levels are occupied. The ratio of the oscillator strengths, S_2/S_3, then is reduced from its value near 1, 0.9, in α-Al_2O_3, by

occupation of the e_g^π states. This ratio is 0.05 in Cr_2O_3 and 0.58 in Ti_2O_3. The intermediate value in Ti_2O_3 is explained by partial occupation of the e_g^π states through thermal excitation across the $a_{1g} - e_g^\pi$ gap.

This argument can also be carried over to a comparison of the A_{2u} modes. In this case the relative oscillator strengths are very nearly the same in Ti_2O_3 and Cr_2O_3, $S_1/S_2 \sim 0.2-0.3$, but are markedly different in α-Al_2O_3, $S_1/S_2 \sim 4$. Referring to Fig. 4, we note that the a_{1g} levels are occupied in Cr_2O_3 and Ti_2O_3 (but not in α-Al_2O_3). These comparisons in the relative oscillator strengths are of course qualitative. A model for the effects of dipole-dipole interactions involving the transition-metal d states is then needed before further quantification is possible.

From the discussion above it is clear that the properties of phonons in α-corundum structured crystals require more study. A rigid-ion model has been appled to α-Al_2O_3 with only modest success.[25] It is evident that more sophisticated lattice dynamical calculations are necessary before we can understand all of the phonon properties. For Ti_2O_3 and the other transition metal sesquioxides, these models must include the coupling of electronic and vibrational excitations as well as the screening introduced by any free carriers.

Other interesting properties are also associated with the long-wavelength phonon states. For example, the large values of the lattice polarizability in Ti_2O_3 suggest that optic phonons may contribute to the scattering of the mobile charge carriers,[26,27] at least for temperatures in the vicinity of room temperature and above. Interactions involving these phonons may also play an important role in the semiconductor-metal transition, even if the electron-lattice interaction does not drive the transition.[28,29] It has been further suggested that large, temperature-dependent anharmonicities in some phonon modes are responsible for piezoresistance extrema[3] in the vicinity of the electrical transition (400–500°K). An examination of Table I does not show any significant differences between the damping of corresponding modes in Ti_2O_3 and in α-Al_2O_3,[6] or Cr_2O_3.[8] Therefore, we find no evidence for large phonon anharmonicities in Ti_2O_3 just above room temperature. This is in agreement with the observation that phonon anharmonicities deduced from ultrasonic attenuation[2] and piezoresistance[3] become important only at significantly higher temperatures in the vicinity of the electrical transition.

In summary then, we have studied the room temperature ir reflectance of Ti_2O_3 for the two principal polarizations and (i) have identified the properties of the six ir-active phonons, $2A_{2u}+4E_u$, (ii) have shown that the optical conductivity, extrapolated to $\nu \to 0$, shows the same anisotropy as the dc conductivity, and (iii) have identified a new interband transition for $\vec{E} \perp \vec{c}$ that gives additional support to the one-electron scheme previously proposed for the Ti $3d$ levels.[12,13] We have compared the properties of the ir-active phonons of Ti_2O_3, with those of α-Al_2O_3 and Cr_2O_3, demonstrating that differences relative to α-Al_2O_3, can be related to the occupancy of energy levels derived from the transition-metal d states.

Note added in proof. Recently infrared reflectance spectra have been reported for yet another crystal with the α-corundum structure, α-Fe_2O_3.[30] The relative oscillator strengths of the ir-active phonons are consistent with the model proposed in this paper if we note that the five $3d$ electrons in α-Fe_2O_3 occupy e_g^σ, as well as a_{1g} and e_g^π states. For example, the ratio S_1/S_2 for the A_{2u} modes in α-Fe_2O_3 in 5.2 and similar to that of α-Al_2O_3, 4.0. This is attributed to the spherical symmetry of the half-filled d shell, in which contributions to the A_{2u} mode polarizations from the e_g^σ states cancel the contributions from the a_{1g} states. For the E_u modes the situation is more complicated with an S_2/S_3 ratio of 4.1 for α-Fe_2O_3 being very different from that in Cr_2O_3, 0.05, but also larger than that in α-Al_2O_3, 0.90.

ACKNOWLEDGMENTS

We are grateful for very useful discussions G. Lucovsky had with Professor J. B. Goodenough of Oxford University, and N. F. Mott of Cambridge University.

*Sabbatical Scientist on leave from Purdue University.

†Received partial support from NSF Grant Nos. DMR 76-11424 and DMR 76-07889 (MRL Program).

[1]See, for example, J. M. Honig and L. L. VanZandt, Ann. Rev. Mater. Sci. 5, 225 (1975).

[2]T. C. Chi and R. J. Sladek, *Proceedings of the Fifth International Conference on Internal Friction and Ultrasonic in Crystalline Solids*, edited by D. Lenz and K. Lucke (Springer-Verlag, Berlin, 1975), Vol. I, p. 127.

[3]H. L. S. Chen and R. J. Sladek, Bull. Am. Phys. Soc. 11, 1355 (1976).

[4]A. Mooradian and P. M. Raccah, Phys. Rev. B 3, 4253 (1971).

[5]S. H. Shin, R. L. Aggarwal, B. Lax and J. M. Honig, Phys. Rev. B 9, 583 (1974).

[6]A. S. Barker, Jr., Phys. Rev. 132, 1474 (1963).

[7]D. R. Renneke and D. W. Lynch, Phys. Rev. 138, A530 (1965).

[8]G. Lucovsky, R. J. Sladek and J. W. Allen, Phys. Rev. B 16, 4716 (1977).
[9]A. S. Barker, Jr. and J. P. Remeika, Solid State Commun. 8, 1521 (1970).
[10]V. P. Zhuze, D. P. Lukirskii, and G. P. Startsev, Fiz. Tverd. Tela 13, 317 (1971). [Sov. Phys.-Solid State 13, 260 (1971)].
[11]M. S. Kozyreva, V. N. Novikov, and B. A. Tallerchik, Fiz. Tverd. Tela 14, 749 (1972) [Sov. Phys.-Solid State 14, 639 (1972)].
[12]J. B. Goodenough, in *Proceedings of the Tenth International Conference on Physics of Semiconductors*, edited by S. P. Keller, J. C Hensel, and F. Stern (USAEC, Oak Ridge, Tenn. 1970), p. 304.
[13]J. B. Goodenough, in *Progress in Solid State Chemistry*, edited by H. Reiss (Pergamon, Oxford, 1972), Vol. 5, p. 145.
[14]S H. Shin, F. Pollak, T. Halpern, and P. M. Raccah, J. Solid State Chem. 12, 407 (1975).
[15]S. S. M. Lu, S. H. Shin, F. H. Pollak, and P. M. Raccah, in *Proceedings of the Thirteenth International Conference on Physics of Semiconductors*, edited by F. G. Fumi (Tipogravia Marves, Rome, 1977). p. 330.
[16]S. H. Shin, F. H. Pollak, T. Halpern, and P. M. Raccah Solid State Commun. 16, 687 (1975).
[17]J. Onstott and G. Lucovsky, J. Phys.Chem. Solids 31, 2172 (1970).
[18]T. Kurosawa, J. Phys. Soc. Jpn. 16, 1298 (1961); W. Cochran and R. A. Cowley, J. Phys. Chem. Solids 23, 447 (1962).
[19]G. Lucovsky and R. J. Sladek, in Proceedings of the International Conference on Lattice Dynamics, Paris, 1977 (unpublished).
[20]G. Lucovsky, R. M. Martin, and E. Burstein, Phys. Rev. B 4, 1367 (1971).
[21]I. Nebenzahl and M. Weger, Phys. Rev. 184, 936 (1969); Philos. Mag. 24, 1119 (1971).
[22]J. Ashkenazi and T. Chuchem, Philos. Mag. 32, 763 (1975).
[23]J. W. Allen, in *Magnetic Oxides*, edited by D. J. Craik (Wiley, New York, 1975), Part 1, Chap. 7, p. 357.
[24]G. Lucovsky and R. M. White, Phys. Rev. B 8, 660 (1973).
[25]H. Bialas and H. J. Stolz, Z. Phys. B 21, 319 (1975).
[26]J. Yahia and H. P. R. Frederikse, Phys. Rev. 123, 2357 (1961).
[27]S. H. Shin, G. V. Chandrashekhar, R. E. Loehman, and J. M. Honig, Phys. Rev. B 8, 1364 (1973).
[28]H. J. Zeiger, Phys. Rev. B 11, 5132 (1975).
[29]N. F. Mott and L. Friedman, Philos. Mag. 30, 389 (1974).
[30]S. Onari, T. Arai and K. Kudo, Phys. Rev. B 16, 1717 (1977).